

Direct Growth of Compound Semiconductor Nanowires by On-Film Formation of Nanowires: Bismuth Telluride

Jinhee Ham,^{†,||} Wooyoung Shim,^{†,§,||} Do Hyun Kim,[‡] Seunghyun Lee,[†]
Jongwook Roh,[†] Sung Woo Sohn,[†] Kyu Hwan Oh,[‡] Peter W. Voorhees,[§]
and Wooyoung Lee^{*,†}

Department of Materials Science and Engineering, Yonsei University, 134 Shinchon, Seoul 120-749, Korea, Department of Materials Science and Engineering, Seoul National University, Seoul 151-744, Korea, and Department of Materials Science and Engineering, Northwestern University, Evanston, Illinois 60208

Received April 2, 2009; Revised Manuscript Received June 6, 2009

ABSTRACT

Bismuth telluride (Bi_2Te_3) nanowires are of great interest as nanoscale building blocks for high-efficiency thermoelectric devices. Their low-dimensional character leads to an enhanced figure-of-merit (ZT), an indicator of thermoelectric efficiency. Herein, we report the invention of a direct growth method termed On-Film Formation of Nanowires (OFF-ON) for making high-quality single-crystal compound semiconductor nanowires, that is, Bi_2Te_3 , without the use of conventional templates, catalysts, or starting materials. We have used the OFF-ON technique to grow single crystal compound semiconductor Bi_2Te_3 nanowires from sputtered BiTe films after thermal annealing at 350 °C. The mechanism for wire growth is stress-induced mass flow along grain boundaries in the polycrystalline film. OFF-ON is a simple but powerful method for growing perfect single-crystal compound semiconductor nanowires of high aspect ratio with high crystallinity that distinguishes it from other competitive growth approaches that have been developed to date.

Novel nanowire growth methods have been of continual interest in many areas of nanoscience and nanotechnology. There are two reasons for this interest: first, nanowires have unusual and unique physical properties, such as quantum-mechanical confinement effects (QCE)¹ and a high surface-to-volume ratio making them relevant for the development of new devices and sensors.^{2,3} In particular, it is believed that QCE plays a crucial role in improving the thermoelectric properties of materials.^{4,5} Theoretical investigations⁶ have suggested that low-dimensional materials, such as Bi_2Te_3 nanowires may exhibit ZT values much larger than 1.0 as a consequence of both the enhanced thermoelectric power (S) and electrical conductivity (σ) and depressed thermal conductivity (κ), which is in contrast with the corresponding properties of the bulk material.⁷ These predictions have stimulated interest in the development of numerous growth methods^{8–25} to synthesize Bi_2Te_3 nanowires over

the past decade. Second, no simple method has been found to date for fabricating nanowires over large areas with compositions such as Bi_2Te_3 . Generally, the synthesis of bismuth telluride-based nanowires can be divided into two categories, electrodeposition into nanoscale inorganic templates^{8–21} and surfactant-mediated solvothermal techniques.^{22–25} Although electrodeposition into nanoporous templates is an attractive method for producing aligned nanorod arrays and making good electrical contacts, this technique is suboptimal for producing of single crystals providing high charge-carrier mobilities.²⁶ On the other hand, solvothermal techniques typically involve reduction of BiPh_3 and TeCl_4 , or BiCl_3 and tellurium powder in organic solvents in the presence of surfactants.^{22,24} Such techniques for growing Bi_2Te_3 nanowires, however, have required the use of templates, catalysts, or other starting materials. The resultant nanowires were not sufficiently conductive to yield high values of ZT due to a low degree of material crystallinity and, in addition, their low aspect ratio made device fabrication difficult.²⁷ Therefore, developing a novel strategy that allows one to easily grow the desired nanowires with high

* To whom correspondence should be addressed. E-mail: wooyoung@yonsei.ac.kr.

[†] Yonsei University.

[‡] Seoul National University.

[§] Northwestern University.

^{||} These authors equally contributed to this work.

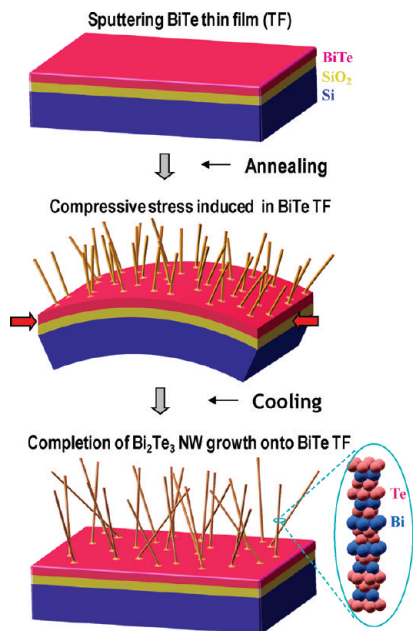


Figure 1. Growth and analysis of Bi_2Te_3 nanowires. Scheme for the growth of Bi_2Te_3 nanowires by OFF-ON: (Step 1) Deposition of BiTe thin films by an UHV dc and rf cosputtering system. (Step 2) Initiating the thermal stress originating from a thermal expansion mismatch between the film and the substrate by annealing at 350 °C for 10 h. (Step 3) Completion of Bi_2Te_3 nanowire growth by releasing the compressive stress after annealing.

crystallinity and high aspect ratio in a simple manner could provide valuable tool to explore their unique properties.

Here, we describe a novel method called on-film formation of nanowires (OFF-ON) for the growth of high-quality, single-crystalline compound semiconductor Bi_2Te_3 nanowires. This novel growth method yields Bi_2Te_3 nanowires from BiTe thin films without the use of conventional templates, catalysts, or starting materials. Figure 1 schematically illustrates OFF-ON, showing the origin and driving force for the growth of Bi_2Te_3 nanowires. BiTe thin films were initially deposited onto a thermally oxidized Si (100) substrate using a cosputtering system with a Bi (99.999%) and a Te target (99.99%) under a base pressure of 2×10^{-7} Torr. The total thickness of the BiTe thin films ranged from 400 to 600 Å. Heating a BiTe thin film to 350 °C induces a stress due to the mismatch between the thermal expansion coefficient of the BiTe film ($\sim 13.4 \times 10^{-6}/^\circ\text{C}$) and a SiO_2/Si substrate ($0.5 \times 10^{-6}/^\circ\text{C}/2.4 \times 10^{-6}/^\circ\text{C}$); this difference acts as a thermodynamic driving force for growth during the thermal annealing process. The BiTe film expands when it is annealed at 350 °C, while the substrate restricts the expansion, putting the BiTe film under compressive stress. Therefore, the spontaneous growth of the Bi_2Te_3 nanowires becomes a means of relieving the compressive stress.

Figure 2a shows a scanning electron microscope (SEM) image of Bi_2Te_3 nanowires grown by OFF-ON after annealing at 350 °C for 10 h. Uniform and straight Bi_2Te_3 nanowires with high aspect ratios were found to grow from the surface of the as-sputtered BiTe film. Nanowires grown by OFF-ON were found to be several tens of micrometers in length and a few tens of nanometers in diameter. High-

resolution transmission electron microscopy (HR-TEM) was utilized to investigate the crystal structure of the Bi_2Te_3 nanowires with a diameter of 65 nm (see Figure 2b). The nanowires were found to be uniform in diameter and to have formed a 2–3 nm thick oxide layer on their outer surface. The selected-area electron diffraction (SAED) pattern obtained in the direction perpendicular to the long axis of the nanowire was indexed to the hexagonal lattice of Bi_2Te_3 ($a = 4.385 \text{ \AA}$, $c = 30.483 \text{ \AA}$) with the electron beam direction along the [001] zone axis, demonstrating that the nanowires are a single crystal grown along the (100) direction. Moreover, crystal spacings for (100) and $(\bar{1}20)$ planes were found to be 2.22 and 2.20 Å, respectively, which is in good agreement with a previous study²⁸ that reports values of 2.20 and 2.20 Å for the (100) and (120) planes of Bi_2Te_3 , respectively. These results explicitly show that the composition of the BiTe nanowire is 2:3. A lattice-resolved image also shows that the nanowires are defect-free, high quality, and single-crystalline (see Figure 2b).

The chemical composition of the Bi_2Te_3 nanowires were confirmed by scanning TEM (STEM) and energy dispersive X-ray spectroscopy (EDS). Figure 2c is a TEM image of a Bi_2Te_3 nanowire lying on a carbon-coated Cu TEM grid. The EDS line scan profile, as shown in the inset of Figure 2c, revealed the uniform spatial distribution of Bi and Te elements throughout the nanowire, which is further confirmed by STEM elemental mapping images across the same nanowire (Figure 2d,e). EDS point scanning experiments at arbitrary positions on the nanowire not only quantitatively confirm that Bi and Te are present in an atomic ratio of 42 ± 1 and $58 \pm 1\%$, respectively, which is within the error detection range of 5% for being Bi_2Te_3 composition, but also indicate that the nanowire is the thermodynamically stable Bi_2Te_3 phase²⁹ which was supported by Figure 2b as described above.

Figure 3a,b shows the cross-sectional bright-field and dark-field TEM images, respectively, taken at the bottom of a Bi_2Te_3 nanowire on an annealed BiTe film. In the bright-field TEM image (Figure 3a), it was found that the BiTe film is polycrystalline with a thickness of 40 nm and that the Bi_2Te_3 nanowire is single crystalline with a diameter of 150 nm. The grains in the BiTe film are discernible as bright areas in the corresponding dark-field image (Figure 3b). From the analysis of corresponding electron diffraction patterns (Figure 3c) as indicated in Figure 3b, the grains were found to be oriented along the $\langle 00l \rangle$ directions after heat treatment, which is in good agreement with the results obtained from XRD patterns.³⁰ The Bi_2Te_3 nanowires were also observed to grow along the [110] direction (E,F in Figure 3c), which is consistent with the electron diffraction patterns as shown in Figure 2b.

The inspiration for OFF-ON methodology comes from the study of a problem that has plagued electronic interconnects: the formation of whiskers (or mounds) in metal films, e.g., Sn,³¹ In,³² Zn,³³ Ag,³⁴ Au.³⁵ In the OFF-ON case, the biaxial stress of the film induces Bi and Te atoms to diffuse along the grain boundaries of the film to produce nanowires (see Figure 4). This is because the diffusion potentials of Bi or

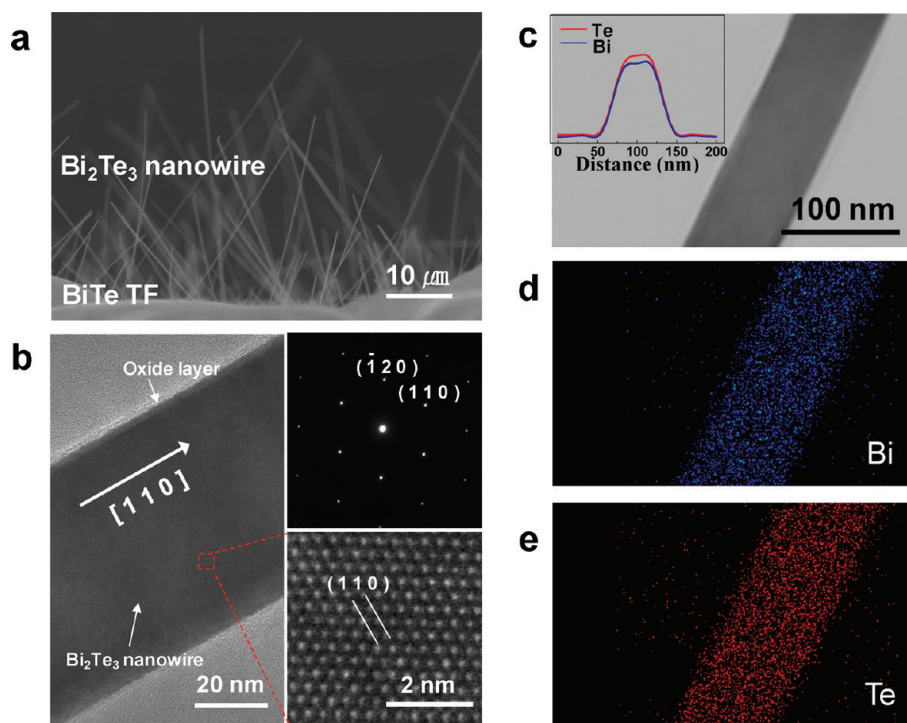


Figure 2. SEM and TEM images of Bi_2Te_3 nanowires. (a) A SEM image of the Bi_2Te_3 nanowires grown on a BiTe thin film: The image shows a side view of the Bi_2Te_3 nanowires that extrude from the surface of the as-sputtered film. (b) A low-magnification TEM image of a Bi_2Te_3 nanowire: the SAED pattern (top right) of the nanowire along the [001] zone axis indicates that the growth direction of the nanowire is [110], and a high-resolution TEM image (bottom right) of the Bi_2Te_3 nanowire shows a perfect single-crystalline material without defects. (c) The scanning TEM (STEM) image of a Bi_2Te_3 nanowire of 80 nm in the diameter. The line profiles show the Bi (blue) and Te (red) homogeneously distributed through the nanowire (inset). (d,e) Elemental mapping showing the uniform distribution Bi (blue, 40.06%) and Te (red, 59.36%) along the length of nanowire.

Te, defined as the chemical potential of Bi or Te minus the chemical potential of a vacancy, at a grain boundary are functions of the normal stress on the boundary.³⁶ Because of the biaxial stress of the film, the diffusion potential is a function of the angle that the boundary makes with the substrate normal, thus the grain boundaries with normals perpendicular to the substrate have the highest diffusion potential and those with normals parallel to the substrate the lowest. Bi and Te atoms thus flow from boundaries that are perpendicular to the substrate normal to those that are inclined with respect to the substrate normal. Atoms do not flow to the surface of the film, even though it has the lowest diffusion potential, since it is covered with a layer of oxide and thus cannot act as a source of vacancies. As emphasized in Boettinger et al.,³⁷ in addition to this mass flow process these inclined boundaries must also be immobile. If the inclined boundaries can move, as illustrated in Figures 4a–c, the result is a mound instead of a wire. In contrast if the inclined boundaries are pinned, a wire is formed; see Figure 4d–f. This mechanism is supported by Figure 3d that shows a cross-section of the root of a Bi_2Te_3 nanowire along with the BiTe thin film. The v-shaped root of the nanowire is bounded by grain boundaries. This morphology is strikingly similar to that seen in much larger Sn-whiskers.^{37,38} Because of the low mobility of the boundaries, for example, resulting from impurity segregation, the boundaries do not move and a wire forms. Consistent with this mechanism, hillocks are also observed in other locations in the sample since not all

inclined boundaries are pinned. The OFF-ON growth process thus requires a polycrystalline film with most of the grains in the film having a columnar morphology and grains that are both noncolumnar and pinned. The number density of the wires will be related to the number density of pinned noncolumnar grains and the diameter of the wires is related to the diameter of these noncolumnar grains.³⁹ Since the temperature at which the wires are grown is above the melting point of pure Bi and above 0.8 of the melting point of pure Te, atoms diffuse easily along the grain boundaries to feed the growth of the wire.

Our previous study has shown that the OFF-ON technique can be used to grow high quality single-crystal Bi wires.³⁹ The present results show that the OFF-ON technique can be used to grow wires with a different composition than the film. The deposited film has an equiatomic composition of Bi and Te, yet the wire has a composition of Bi_2Te_3 . The Bi_2Te_3 phase has the highest melting point of any Bi–Te compound and thus it likely has a large thermodynamic driving force for nucleation. Its presence indicates that the Bi_2Te_3 nucleation and growth kinetics are sufficiently rapid for it to form wires.

Since an oxide layer of 2–3 nm on a Bi_2Te_3 nanowire (see Figure 2C) prevents good electrical measurements from being taken, we employed a focused ion beam (FIB) system to make ohmic contacts to a Bi_2Te_3 nanowire. This was done by first sputtering off the oxide layer and then depositing platinum by introducing Pt-hydrocarbon gas (methylcyclo-

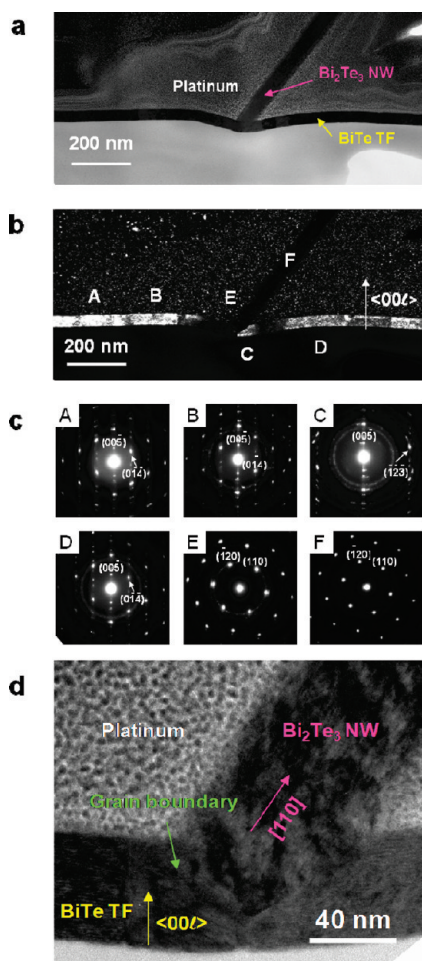


Figure 3. TEM study of the cross-section of a Bi_2Te_3 nanowire– BiTe thin film. (a) Bright field TEM image of a Bi_2Te_3 nanowire– BiTe thin film. BiTe thin film consists of grains which look like a bamboo-like structure. (b) Dark-field TEM image of Bi_2Te_3 nanowire– BiTe thin film. The image shows the oriented $\langle 00l \rangle$ direction of grains in the BiTe thin film as indicated in XRD analysis. (c) SAED patterns at A, B, C, D, E, and F in Figure 4b. A–D show the oriented $\langle 00l \rangle$ direction of grains in the BiTe thin film. E and F show the oriented (100) direction of Bi_2Te_3 nanowire on BiTe thin film. (d) The high-resolution TEM image of the grown Bi_2Te_3 nanowire on the BiTe thin film. Bi_2Te_3 nanowires grow at the grain boundary of the BiTe thin film.

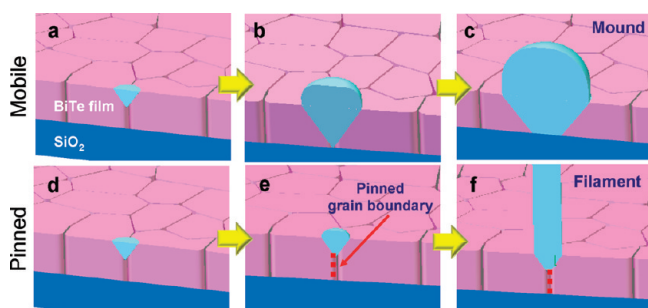


Figure 4. Schematics of different response of surface grains to the biaxial stress depending on the mobility of the grain boundary. (a–c) The surface grain broaden laterally by grain boundary migration as it is pushed upward, thus spread over a large surface. (d–f) The grain base broadening is hindered since inclined boundaries are pinned, therefore the upward motion of Bi and Te is concentrated into contorted filamentary whisker.

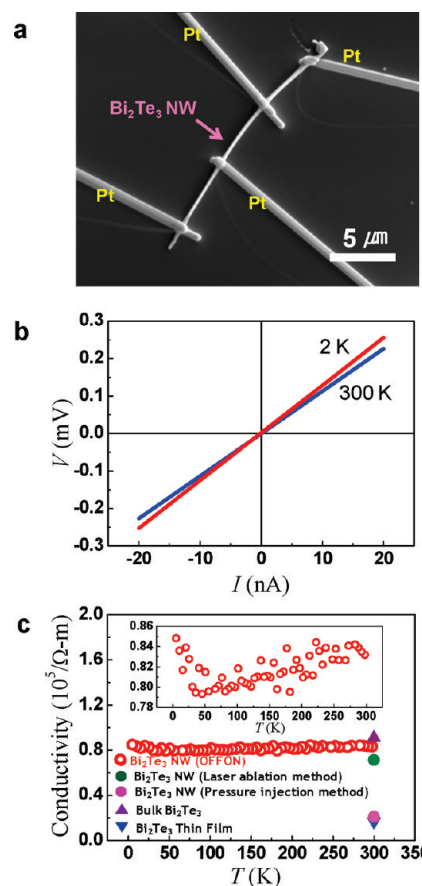


Figure 5. Device based on an individual Bi_2Te_3 nanowire to investigate its transport properties. (a) Four-terminal device based on an individual Bi_2Te_3 nanowire. (b) I – V measurement showing good ohmic contact. The resistivities are 1.1×10^{-3} and $9.79 \times 10^{-4} \Omega\cdot\text{cm}$ at temperatures of 2 and 300 K, respectively. (c) The electrical conductivity of the Bi_2Te_3 nanowire from 300 to 2 K. The conductivity of the Bi_2Te_3 nanowire with OFF-ON is higher than that of Bi_2Te_3 nanowires made by laser ablation method, bulk Bi_2Te_3 or Bi_2Te_3 thin film.

pentadienyl) in the path of the Ga-ion beam. Both steps were carried out in situ without breaking vacuum. Once the oxide had been removed from the nanowire in the contact areas, a small amount of Pt-hydrocarbon gas was introduced above the sample, and Pt electrodes were deposited by rastering the Ga-ion beam to form the electrode pattern. A SEM image of a 77 nm Bi_2Te_3 nanowire prepared using this technique is presented in Figure 5a. The four sticklike lines are the Pt electrodes and the strips attached to the Pt wires are gold electrodes, which in turn are attached to four large bonding pads patterned by photolithography. From I – V measurements, the contacts to the nanowire were observed to be highly ohmic at both 2 and 300 K (Figure 5b), corresponding to conductivities, σ , of 0.77×10^3 and $0.86 \times 10^3 \Omega^{-1}\cdot\text{cm}^{-1}$, respectively. The observed conductivity for the 86 nm diameter Bi_2Te_3 nanowire at room temperature is slightly lower than that of bulk ($\sigma_{\text{bulk}} = 0.9 \times 10^3 \Omega^{-1}\cdot\text{cm}^{-1}$)⁷ but notably higher than that of thin film ($\sigma_{\text{film}} = 0.17 \times 10^3 \Omega^{-1}\cdot\text{cm}^{-1}$),⁴⁰ pressure injected nanowires ($\sigma_{\text{nanowire}} = 0.21 \times 10^3 \Omega^{-1}\cdot\text{cm}^{-1}$),¹⁸ and laser-ablated nanowires ($\sigma_{\text{nanowire}} = 0.71 \times 10^3 \Omega^{-1}\cdot\text{cm}^{-1}$)⁴¹ by 406, 310, and 21%, respectively. Our results support the view that the Bi_2Te_3 nanowires grown

by OFF-ON are high-quality single crystalline, as corroborated by high-resolution TEM in Figure 2b.

The temperature dependence of conductivity $\sigma(T)$ for the individual 77 nm diameter Bi_2Te_3 nanowire in the temperature range 2–300 K is shown in Figure 5c. The electrical conductivity for the nanowire was observed to be the higher than previously reported values^{7,18,40,41} (see Figure 5c), indicative of the high-quality crystallinity of the Bi_2Te_3 nanowires grown using OFF-ON. It was found that σ increased with increasing T from 2 to 46 K, while $\sigma(T)$ decreased with increasing T above 46 K. The increase of σ in the range $2 < T < 46$ K is attributable to the nature of semiconductors where charge carriers are thermally excited, thus σ increases with T . In general, intrinsic semiconductors require high temperature to generate electron–hole pairs via thermal excitation mechanisms. Therefore, total carrier concentrations are mostly invariant at low temperature. Bi_2Te_3 , however, possesses a narrow band gap (0.2 eV), and thus it is expected that very little thermal energy ($50 < T < 100$ K) is required to generate the charge carriers as seen in extrinsic materials with additional levels within the band gap.⁴² Consequently, carrier concentrations will increase as T increases even in the low temperature regime, giving rise to an increase of σ . Thus at low temperatures, all of the carriers are generated, leading to the fact that $\sigma(T)$ exhibits a decrease with further increasing T due to the increasing contribution of electron–phonon scattering.

In conclusion, we have developed a new growth method termed OFF-ON to generate perfect single-crystal, compound semiconductor Bi_2Te_3 nanowires in a simple manner using the thermally induced stress of a thin film. The technique merges many of the attributes of a simple sputtering method and thermal annealing to yield defect-free high-aspect ratio nanowires with high throughput. The simple requirements for the growth of the wire are atomic diffusion of Bi and Te along grain boundaries in the presence of compressive stress, and these have significant implications for extending OFF-ON to other material systems. Our results show that Bi_2Te_3 wires grown by OFF-ON yield the high quality single crystals and high conductivity of relevance for high efficiency thermoelectric devices.

Acknowledgment. This work was supported by a grant from “Center for Nanostructured Materials Technology” under “21st Century Frontier R&D Programs” of the Ministry of Education, Science and Technology and by KOSEF through National Core Research Center for Nanomedical Technology (R15-2004-024-00000-0) and by Seoul Research and Business Development Program (10816). K.H.O. acknowledges the support of the Korea Science and Engineering Foundation (KOSEF) grants (No. R11-2005-065, Chung and No. R01-2007-000-10032-0). P.W.V. is grateful for the financial support of the National Science Foundation, DMI-0507053. J.H.H. thanks the financial support of the Seoul Science Fellowship.

Supporting Information Available: This material is available free of charge via the Internet at <http://pubs.acs.org>.

References

- (1) Holmes, J. Control of thickness and orientation of solution-grown Si nanowires. *Science* **2000**, *287*, 1471–1473.
- (2) Wang, J. Nanomaterial-based electrochemical biosensors. *Analyst* **2005**, *130*, 421–426.
- (3) Ng, H. Growth of epitaxial nanowires at the junctions of nanowalls. *Science* **2003**, *300*, 1249.
- (4) Dresselhaus, M. Low-dimensional thermoelectric materials. *Phys. Solid State* **1999**, *41*, 679–682.
- (5) Hicks, L. Thermoelectric figure of merit of a one-dimensional conductor. *Phys. Rev. B* **1993**, *47*, 16631–16634.
- (6) Dresselhaus, M. The promise of low-dimensional thermoelectric materials. *Microscale Thermophys. Eng.* **1999**, *3*, 89–100.
- (7) Rowe, D. *Thermoelectrics handbook: Macro to nano*; Taylor & Francis: New York, 2006.
- (8) Prieto, A. Electrodeposition of ordered Bi_2Te_3 nanowire arrays. *J. Am. Chem. Soc.* **2001**, *123*, 7160–7161.
- (9) Sander, M. Structure of bismuth telluride nanowire arrays fabricated by electrodeposition into porous anodic alumina templates. *Chem. Mater.* **2003**, *15*, 335–339.
- (10) Wang, W. Investigation of electrodeposition of Bi_2Te_3 nanowires into nanoporous alumina templates with a rotating electrode. *J. Phys. Chem. B* **2006**, *110*, 12974–12980.
- (11) Trahey, L. Electrodeposited bismuth telluride nanowire arrays with uniform growth fronts. *Nano Lett.* **2007**, *7*, 2535–2539.
- (12) Gonzalez, M. Direct electrodeposition of highly dense 50 nm $\text{Bi}_2\text{Te}_{3-y}\text{Se}_y$ nanowire arrays. *Nano Lett.* **2003**, *3*, 973–977.
- (13) Gonzalez, M. High-density 40 nm diameter Sb-rich $\text{Bi}_{2-x}\text{Sb}_x\text{Te}_3$ nanowire arrays. *Adv. Mater.* **2003**, *15*, 1003–1006.
- (14) Gonzalez, M. Electrodeposition of $\text{Bi}_{1-x}\text{Sb}_x$ films and 200 nm wire arrays from a nonaqueous solvent. *Chem. Mater.* **2003**, *15*, 1676–1681.
- (15) Sander, M. Fabrication of high-density, high aspect ratio, large-area bismuth telluride nanowire arrays by electrodeposition into porous anodic alumina templates. *Adv. Mater.* **2002**, *14*, 665–667.
- (16) Gonzalez, M. Insights into the electrodeposition of Bi_2Te_3 . *J. Electrochem. Soc.* **2002**, *149*, C546–C554.
- (17) Menke, E. Bismuth telluride (Bi_2Te_3) nanowires synthesized by cyclic electrodeposition/stripping coupled with step edge decoration. *Nano Lett.* **2004**, *4*, 2009–2014.
- (18) Jones, P. Electrical contact resistance of bismuth telluride nanowires. *Int. Conf. Thermoelectr.* **2006**, 693–696.
- (19) Cronin, S. *International Conference on Thermoelectrics* **1999**, 554–557.
- (20) Li, D.; et al. Measurement of Bi_2Te_3 nanowire thermal conductivity and seebeck coefficient. *Int. Conf. Thermoelectr.* **1999**, 554–557.
- (21) Zhou, J.; et al. Thermoelectric properties of individual electrodeposited bismuth telluride nanowires. *Appl. Phys. Lett.* **2005**, *87*, 133109.
- (22) Yu, H. Bismuth, tellurium, and bismuth telluride nanowires. *J. Mater. Chem.* **2004**, *14*, 595–602.
- (23) Purkayastha, A. Low-temperature, template-free synthesis of single-crystal bismuth telluride nanorods. *Adv. Mater.* **2006**, *18*, 496–500.
- (24) Deng, Y. Organic-assisted growth of bismuth telluride nanocrystals. *Chem. Phys. Lett.* **2003**, *374*, 410–415.
- (25) Ji, X. Solvothermal preparations of nanocrystalline Bi_2Te_3 powders and the study on their characterizations. *Mater. Res. Soc. Symp. Proc.* **2004**, *793*, S1.4.1.
- (26) Chen, G. Recent developments in thermoelectric materials. *Int. Mater. Rev.* **2003**, *48*, 45–66.
- (27) Zhou, J. Measurement of thermoelectric properties of individual bismuth telluride nanowires. *Int. Conf. Thermoelectr.* **2005**, 17–20.
- (28) *Natl. Bur. Stand. (U.S.) Monogr.* **1964**, *25* (3), 16.
- (29) Hansen, M.; Anderko, K. *Constitution of binary alloys*; McGraw-Hill: New York, 1958; p 339.
- (30) See Supporting Information.
- (31) Tu, K. Cu/Sn interfacial reactions: thin-film case versus bulk case. *Mater. Chem. Phys.* **1996**, *46*, 217–223.
- (32) Damascchke, B. Inverse AC Josephson effect in superconducting In and Pb whiskers. *Phys. Rev. B: Condens. Matter* **1989**, *77*, 17–23.
- (33) Brusse, J.; Sampson, M. Zinc whiskers: hidden cause of equipment failure. *IEEE IT Professional Magazine* **2004**, *6*, 43–47.
- (34) Chudnovsky, B. Degradation of power contacts in industrial atmosphere: silver corrosion and whiskers. *48th IEEE Holm Conference on Electrical Contacts* **2002**, 140–150.
- (35) Teverovsky, A. Introducing a new member to the family: gold whiskers. *Internal NASA Goddard Space Flight Center Memorandum*, 2003, pp 1–6.

- (36) Herring, C. The Diffusional Viscosity of a Polycrystalline Solid. *J. Appl. Phys.* **1950**, *21*, 437–445.
- (37) Boettinger, W. J.; Johnson, C. E.; Bendersky, L. A.; Moon, K.-W.; Williams, M. E.; Stafford, G. R. Whisker and Hillock formation on Sn, Sn-Cu, and Sn-Pb electrodeposits. *Acta Mater.* **2005**, *53*, 5033–5050.
- (38) Hutchinson, B; Oliver, J; Nyle'n, M.; Hagström, M. Recrystallization and grain growth. *J. Mater. Sci. Forum* **2004**, *465*, 467–470.
- (39) Shim, W.; Ham, J.; Lee, K.; Jeung, W.; Johnson, M.; Lee, W. On-film formation of Bi nanowires with extraordinary electron mobility. *Nano Lett.* **2009**, *9* (1), 18–22.
- (40) Das, V.; Soundararajan, N. Size and temperature effects on the thermoelectric power and electrical resistivity of bismuth telluride thin films. *Phys. Rev. B* **1988**, *37*, 4552–4559.
- (41) Wei, Q.; Lieber, C. Synthesis of single crystal bismuth telluride and lead telluride nanowires for new thermoelectric materials. *Mater. Res. Soc. Symp. Proc.* **2000**, *581*, 219–223.
- (42) Streetman, B; Banerjee, S. *Solid state electronic devices*; Pearson Prentice Hall: NJ, 2006.

NL9010518